Modeling and Validation of Mobility Characteristics of the Mars Science Laboratory Curiosity Rover

C. Senatore*, N. Stein**, F. Zhou**, K. Bennett**, R. E. Arvidson**, B. Trease***, R. Lindemann***, P. Bellutta***, M. Heverly***, K. Iagnemma*

*Laboratory for Manufacturing and Productivity, MIT, USA
e-mail: senator@mit.edu, kdi@mit.edu

**Earth and Planetary Remote Sensing Laboratory, University of Washington in St. Louis, USA
e-mail:n.stein@wustl.edu, chow@wunder.wustl.edu, bennett@wustl.edu, arvidson@wunder.wustl.edu

***Jet Propulsion Laboratory, NASA, USA
e-mail: brian.p.trease@jpl.nasa.gov, randel.a.lindemann@jpl.nasa.gov, bellutta@helios.jpl.nasa.gov, matthew.c.heverly@jpl.nasa.gov

Abstract

This paper describes recent work toward developing a terramechanics-based modeling and validation infrastructure for characterizing the Curiosity rovers mobility properties on the Mars surface. The resulting simulation tool, ARTEMIS (Adams-based Rover Terramechanics and Mobility Interaction Simulator), is composed of a MSC-Adams dynamic rover model, a library of terramechanics subroutines, and high-resolution digital elevation maps of the Mars surface.

Rover-terrain interactions that are modeled include longitudinal, lateral, and vertical wheel-terrain interaction forces, the effect of slip sinkage, and multi-pass effects. A single wheel ARTEMIS model was also developed. Model validation has been performed via several complementary methods. Mobility properties of a Curiosity rover flight spare wheel have been analyzed at the Robotic Mobility Groups terramechanics lab at MIT using a single wheel test rig capable of reproducing forced-slip and free-slip conditions. In order to evaluate ARTEMIS potential in full, the simulation was used to model the performance of the Mars-weight Curiosity test rover (a.k.a. Scarecrow) while operating in realistic scenarios.

1 Introduction

The Mars Science Laboratory (MSL) Curiosity rover successfully landed on Mars on the plains of Gale crater on August 6th 2012 [5]. From a mobility standpoint, the ongoing mission has thus far encountered mostly benign plains composed of soil-covered surfaces with embedded rock clasts, together with some bedrock outcrops [2]. However, it is likely that Curiosity will face more challenging terrains when crossing the longitudinal and barchan dunes to get to Mount Sharp and during the ascent of Mount Sharp, which contains steeply sloped terrain and bedrock surfaces covered by loose, sandy soils of varying depth.

Realistic simulations of rover-terrain interactions during traverses are needed to help engineers define safe and efficient paths to waypoints for robotic systems such as Opportunity and Curiosity. A spin-off of such a capability is that the rover can also be used as a virtual instrument, sensing the terrain slope distributions, together with soil and bedrock properties. Registration of model and flight data can be used to retrieve surface properties and also increase the confidence with which future traverse path options can be simulated.

This paper describes recent work toward developing a terramechanics-based modeling and validation infrastructure for characterizing the Curiosity rovers mobility properties on the Mars surface. The resulting simulation tool, ARTEMIS (Adams-based Rover Terramechanics and Mobility Interaction Simulator), is composed of a MSC-Adams dynamic rover model, a library of terramechanics subroutines, and high-resolution digital elevation maps of the Mars surface [11]. Rover-terrain interactions that are modeled include longitudinal, lateral, and vertical wheel-terrain interaction forces, the effect of slip sinkage, and multi-pass effects. ARTEMIS has previously been successfully employed to model MER rover mobility properties [11, 1].

The paper is organized as follows. Section 2 briefly introduces ARTEMIS; section 3 presents the MSL single wheel terramechanics test bed; section 4 describes the regolith simulants utilized for this study; section 5 shows single wheel forced-slip and free-slip experiments and full vehicle experiments on inclined terrains.

2 ARTEMIS

ARTEMIS (Adams-based Rover Terramechanics and Mobility Interaction Simulator), is composed of a MSC-Adams dynamic rover model, a library of terramechanics subroutines, and high-resolution digital elevation maps of the Mars (or other candidate terrains) surface. Rover-terrain interactions that are modeled include longitudinal, lateral, and vertical wheel-terrain interaction forces, the effect of slip sinkage, and multi-pass effects. ARTEMIS is able to handle interactions with soft soil (i.e., regolith) and hard terrains (i.e., bedrocks, flagstones, etc.). For the deformable soil interaction model, formulations are based on the traditional terramechanics theory by Bekker and Wong [3, 10].

To facilitate understanding of the parameters discussed in this paper, a brief introduction of the key terramechanics formulations is presented here. ARTEMIS has previously been successfully employed to model MER rover mobility properties and more details on the terramechanics subroutine can be found in [11, 1]. The model relies on terramechanics relations first developed by Bekker and later modified by Wong and Reece [wong67a,wong67b]. Figure 1 indicates the chosen coordinate frame and introduces a schematic representation of the stresses acting on the wheel.

The normal stress at the wheel-terrain contact patch is assumed to be purely radial, and is calculated using the Wong and Reece equation [wong67a]

$$\begin{aligned} \sigma &= \begin{cases} \sigma_1 = \psi z_1^n & \theta_m < \theta < \theta_f \\ \sigma_2 = \psi z_2^n & \theta_r < \theta < \theta_m \end{cases} \\ z_1 &= r(\cos\theta - \cos\theta_f) \\ z_2 &= r\left(\cos\left(\theta_f - \frac{\theta - \theta_r}{\theta_m - \theta_r}(\theta_f - \theta_m)\right) - \cos\theta_f\right) \end{aligned} \quad (1)$$

where θ_f is the soil entry angle, θ_r is the exit angle, θ_m is the angle at which the maximum normal stress occurs, and r is the wheel radius (see Figure 1). ARTEMIS can utilize either Bekker or Reece pressure-sinkage formulation:

$$\psi = \begin{cases} \frac{k_c}{b} + k_\phi & Bekker \\ ck'_c + \rho g b k'_\phi & Reece \end{cases} \quad (2)$$

Parameters k_c, k_ϕ, n, k'_c, k'_ϕ depend on soil properties, while g is gravity, ρ is terrain density, and b corresponds to the smallest dimension between the wheel width and contact patch length. To better model slip-sinkage effects the sinkage exponent n is expressed as function of slip as follows:

$$n = n_0 + n_1 i \quad (3)$$

where n_0 is the nominal sinkage exponent and n_1 is the slip-sinkage exponent, which is determined empirically [4]. The angle at which the maximum normal stress occurs can be calculated as:

$$\theta_m = (a_1 + a_2 i)\theta_f \quad (4)$$

The wheel is divided into "slices" normal to the axis of rotation and the entry and exit angle are calculated for each slice. The normal stress in each patch is computed independently. Shear stress in the longitudinal direction (i.e. the direction of travel) is the primary source of driving traction. Shear stress is function of soil parameters and the measured shear deformation, j:

$$\tau = (c + \sigma tan\phi)\left(1 - e^{-\frac{j}{k_x}}\right) \quad (5)$$

where c is the soil cohesion, ϕ is the angle of internal friction, k_x is the shear modulus (a measure of shear stiffness), and j is shear deformation:

$$j = \int_0^{t_0} v_t d\theta = \int_\theta^{\theta_f} v_t \frac{d\theta}{\omega} \quad (6)$$

where v_t is the tangential slip velocity and k_x is the shear modulus.

Traction forces generated by a wheel can be decomposed in two components: a thrust component, which acts to move the vehicle forward; and a compaction resistance component, which resists forward motion. Thrust, T, is computed as the sum of all shear force components in the direction of forward motion:

$$T = br \int_{\theta_r}^{\theta_f} \tau \cos\theta d\theta \quad (7)$$

Compaction resistance, R_c, is the result of all normal force components acting to resist forward motion, and can be thought of as the net resistance force provided by the soil:

$$R_c = br \int_{\theta_r}^{\theta_f} \sigma \sin\theta d\theta \quad (8)$$

The net longitudinal force, also termed the drawbar pull, is calculated as the difference between the thrust force and resistance force. DP is the resultant force that can provide a pulling/braking force at the vehicle axle.

$$DP = T - R_c + F_g \quad (9)$$

where F_g is the thrust produced by grousers. More detail about grousers force calculation can be found in [11].

The importance of drawbar force is obvious, since a positive drawbar force implies that a rover can generate forward motion on a particular patch of terrain, while a negative drawbar force suggests that forward motion is difficult or impossible. Torque, M, is the resultant of shearing action along wheel rim, and can be calculated as:

$$M = br^2 \int_{\theta_r}^{\theta_f} \tau d\theta \quad (10)$$

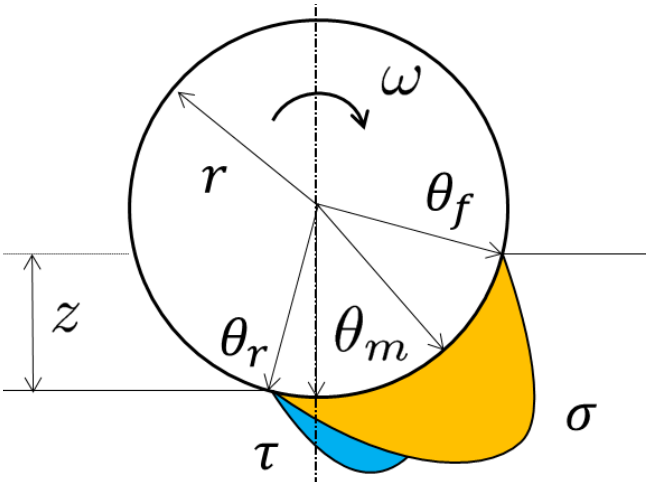

Figure 1. Schematic representation of normal and tangential stress profile along the wheel-soil interface.

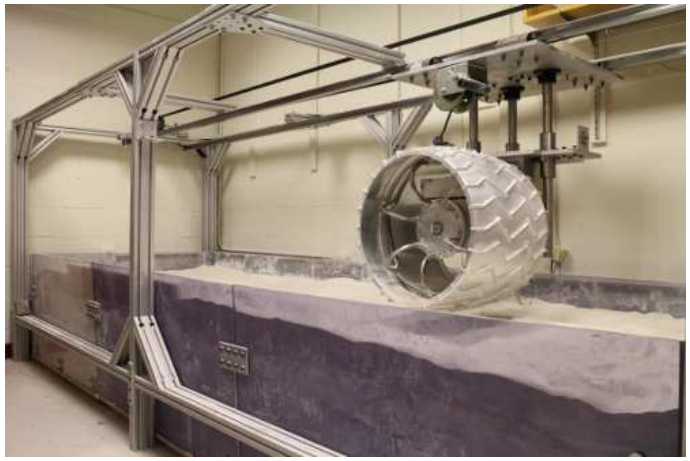

Figure 2. MSL terramechanics test bed at MIT. This rig allows for forced-slip and free-slip tests.

3 Single Wheel Test Bed

The Robotic Mobility Group at MIT has designed and fabricated a multi-purpose terramechanics rig based on the standard design described by Iagnemma [7]. The test bed is pictured in Figure 2 and it is composed of a Lexan soil bin surrounded by an aluminum frame where all the moving parts, actuators and sensors are attached. A carriage slides on two linear bearings to allow longitudinal translation while the wheel, attached to the carriage, is able to rotate at a desired angular velocity. The wheel mount is also able to freely translate in the vertical direction. This typical setup allows control of slip and vertical load by modifying the translational velocity of the carriage, angular velocity of the wheel, and applied load. Alternatively, it is possible to disconnect the longitudinal drive system and actuate the wheel independently, hence recreating free-slip conditions.

Horizontal carriage displacement is controlled through a toothed belt actuated by a 200 W Maxon DC motor, while the wheel is directly driven by a 250 W Maxon DC motor. The motors are controlled through two identical Maxon ADS 50/10 4-Q-DC servo-amplifiers. The carriage horizontal displacement is monitored with a Micro Epsilon MK88 draw wire encoder while wheel vertical displacement (i.e., sinkage) is measured with a Turck A50 draw wire encoder.

A 6-axis force torque ATI Omega 160 transducer is mounted between the wheel mount and the carriage in order to measure vertical load and traction generated by the wheel. Finally, a flange-to-flange reaction torque sensor from Futek (TFF600) is used to measure driving torque applied to the wheel. Control and measurement signals are handled by a NI PCIe-6363 card through Labview software.

The rig is capable of approximately 3.5 meters of longitudinal displacement at a maximum velocity of approximately 60 mm/s with a maximal wheel angular velocity of approximately 15 deg/s. The bin width is 1.2 meters while the soil depth is 0.5 meters. Considering the wheel sizes and vertical loads under study, these physical dimensions are sufficient for eliminating boundary effects. Moreover, the same testbed, with some adaptations, can be used to perform soil penetration tests.

4 Test-Bed Soils

The experiments presented in this paper are conducted on two different types of dry granular materials. For the single wheel experiments, performed at MIT, a new simulant has been developed from commercially available sands. This granular material was created with the intent of reproducing grain size distribution and mechanical properties of the most challenging terrains observed on Mars. The simulant is obtained blending of 75% Mauricetown NJ70 sand and 25% SilCoSil250 ground silica (percent represents mass fraction). The resulting mix was tested under direct shear and plate penetration tests to evaluate mechanical properties under different loading conditions.

Direct shear tests showed that the simulant has a shear modulus of 0.001 m, presents a cohesion of 0.43 kPa, and an angle of internal friction of 34 degrees. Direct shear tests were conducted under three different vertical loads repeating each experiment 4 times. Results, presented in Figure 3, show little variation between each trial.

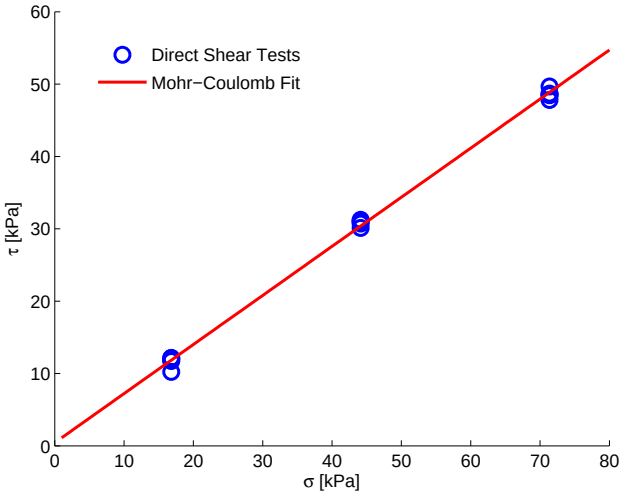

Figure 3. Mohr-Coulomb failure envelope for the MIT sand.

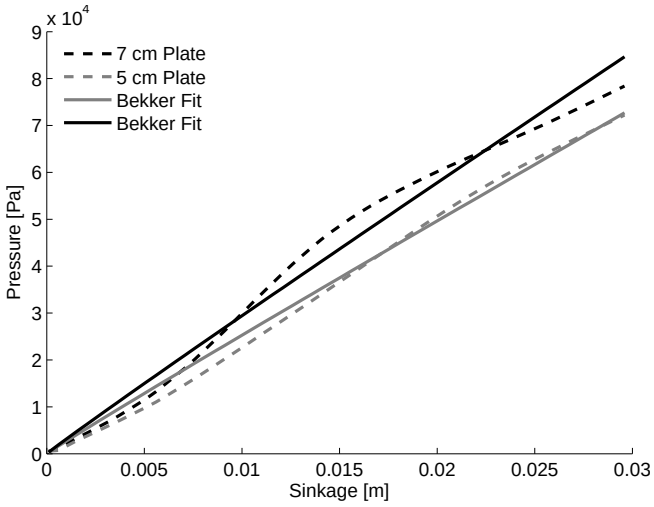

Figure 4. Pressure-sinkage characteristics of the MIT sand.

Table 1. Mechanical properties of the MIT sand measured through direct shear and plate penetration tests.

Symbol	Value	Units
n	1.26	n/a
k_c	-404	kN/m^{n+1}
k_ϕ	15500	kN/m^{n+2}
c	430	Pa
ϕ	35	deg
k_x	0.001	m

The simulant was also tested under penetrating plates in order to extrapolate Bekker pressure-sinkage parameters. The experiments were conducted with two plates of 0.05 m x 0.16 m and 0.07 m x 0.16 m area. For each plate 15 repetitions were conducted and the fit was conducted on the average of the 15 trials, as shown in Figure 4. MIT regolith simulant properties are summarized in Table 1.

The Dumont Dunes test area in the Mojave Desert is dominated by well-sorted, rounded, wind-blown sands dominated by quartz and feldspar. For the experiments conducted at this site, the topography was characterized using a scanning laser altimeter. Soil properties were not determined but rather treated as an unknown, and ARTEMIS simulations were tuned to achieve best performance.

5 Results

The results are divided in two subsections. Single wheel experiments are compared to ARTEMIS simulations utilizing measured sand parameters first. Then, it is shown how it is possible to use ARTEMIS to characterize in-field tests.

Table 2. MIT sand properties for ARTEMIS simulations.

k_x [m]	n_1	a_1	a_2
0.0146	0.54	0.38	0.44

5.1 Single Wheel Experiments vs. ARTEMIS

Single wheel experiments have been conducted using two testing methodologies: forced-slip and free-slip. For the forced-slip experiments the wheel longitudinal and angular velocities were fully controlled, thus imposing wheel slip during the test. For the free-slip experiments the wheel longitudinal velocity was not constrained, and dead weights were used to increase longitudinal motion resistance. For this experimental setup the slip becomes a free variable.

Results for forced-slip and free-slip experiments are presented in Figures 5, 6, 7. For the forced slip experiments 5 repetitions at each normal load and slip combinations were conducted. Boxplots represent average with the whiskers showing one standard deviation for these experiments. It is evident that torque and drawbar measurements are very repeatable while sinkage shows more variance. This is a consequence of the inability to precisely prepare the surface back to its original topographic state after each run. Experimental data for the free-slip experiments overlap with the forced-slip experiments, which suggests that the two testing methodologies are indeed equivalent.

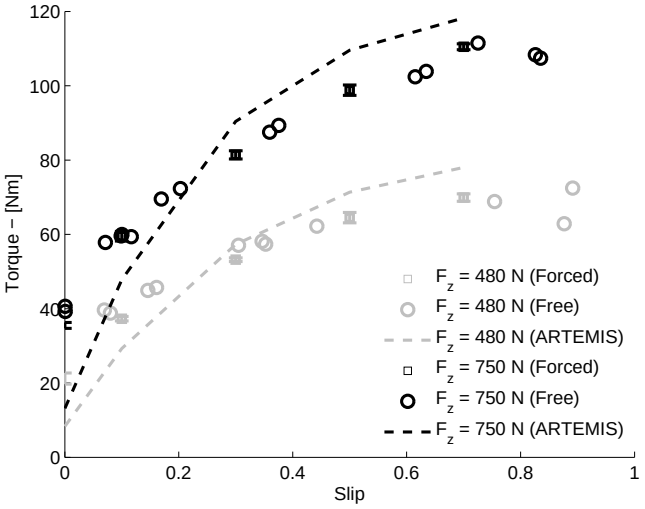

Figure 5. Torque vs. longitudinal slip for ARTEMIS model and single-wheel experimental data.

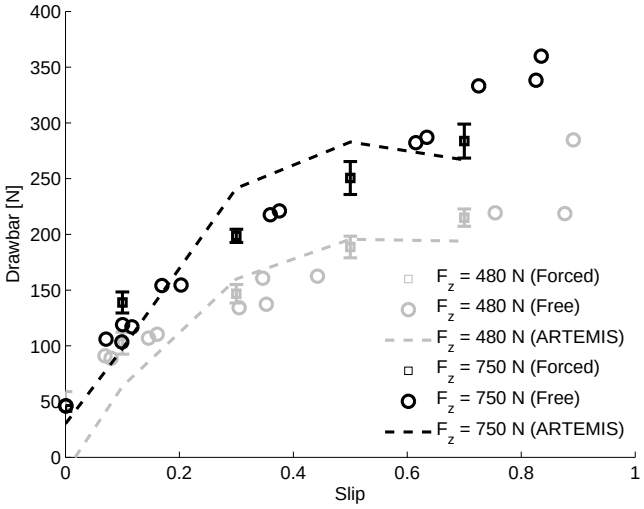

Figure 6. Drawbar vs. longitudinal slip for ARTEMIS model and single-wheel experimental data.

Also, for the free-slip experiments, sinkage shows significant variability.

For the ARTEMIS simulations, the parameters k_x, n_1, a_1 and a_2, were used as tuning parameters while all other parameters were taken from Table 1. More details on the reasons for this approach are presented in [11, 9, 8] while Table 2 shows the values for the tuning parameters.

Single wheel ARTEMIS simulations show good agreement with drawbar and torque measurements while sinkage is underestimated. Although this is not ideal, it reflects the known limitations of semi-empirical terramechanics models. In the next section it will be shown that, notwithstanding its limitations, ARTEMIS can be utilized to characterize full vehicle operations.

5.2 ARTEMIS vs. Field Tests

A series of field tests were conducted at the Dumont Dunes site utilizing the Scarecrow platform [6]. Scarecrow is a fully functional mockup of the rover Curiosity weighting approximately 3/8 of Curiosity in order to reproduce on earth similar ground pressures to the ones experienced on Mars (Figure 8). The Dumont Dunes were selected in the Mojave Desert as wind-blown dune field analogous to wind-blown sand dunes seen from orbit covering a portion of the rovers landing target ellipse on Mars.

An extensive report of these field tests is reported in [6]. In this paper, the focus is on the climbing performance of Scarecrow. The analysis of the rover climbing capabilities is conducted following three approaches:

1. ARTEMIS simulations of the full vehicle.

2. Simplified analysis based on ARTEMIS single wheel simulations including weight transfer effects.

3. Simplified analysis based on ARTEMIS single wheel simulations neglecting weight transfer effects.

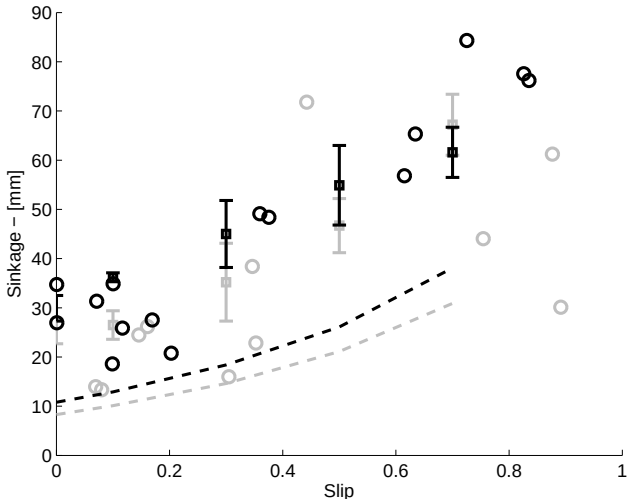

Figure 7. Sinkage vs. longitudinal slip for ARTEMIS model and single-wheel experimental data.

The first approach essentially utilizes the ARTEMIS full vehicle model to replicate the actual drive that the rover performed. This is the most complete analysis and it is also the more computationally intensive. Since soil properties for the Dumont Dunes site were not available this analysis was also utilized to extrapolate terrain properties. Sand properties are obtained from the SSTB-lite

Figure 8. Scarecrow at the Dumont Dunes site while attempting an upslope drive.

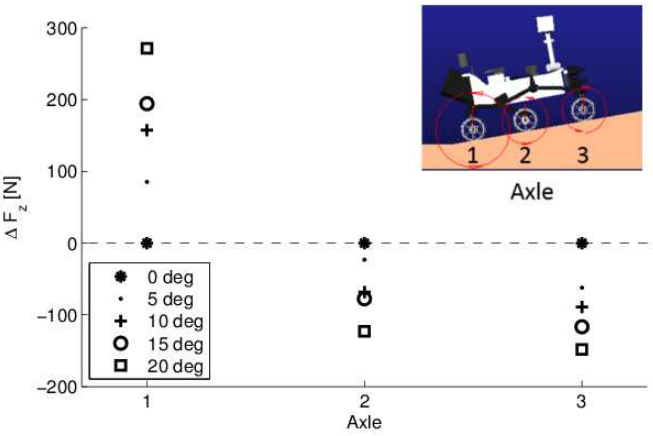

Figure 9. Load transfer during upslope drives. Values represent the additional load that is carried by each wheel. Considering that the nominal load is approximately 550 N, the rear axle can experience up to 50% surcharge during a 20 degrees slope ascent.

rover simulations as presented in [11] and are utilized to model scarecrow drive. Sand properties are summarized in Table 3.

The second approach utilizes single wheel ARTEMIS simulations (conducted on flat ground) and weight transfer information to estimate the amount of slip necessary to drive up a slope of varying grade. Figure 9 shows vertical load distributions for the three axles of the rover once steady state climbing has been reached on slopes of different inclinations. These values have been obtained from the ARTEMIS full vehicle simulation and show how more load is transferred to the rear axle while less is carried by the front axle when the vehicle travels on an incline. Given the vertical load for each wheel it is possible to calculate the slip required to climb by solving:

$$\sum_{n=1}^{6} DP_n(F_{zn}\cos\alpha, i) - F_{zn}\sin\alpha = 0 \qquad (11)$$

where DP_n is the drawbar force at the n-th wheel, F_{zn} is the reaction force under the wheel in the direction parallel to the earth gravity vector, α is the slope inclination, and i is slip. Equation 11 can be solved for slip in order to yield slip vs. inclination curves.

The third approach is similar to the second, but disregards the load transfer and simply assumes that each wheel carries the same amount of load, reducing the analysis to:

$$DP(F_z\cos\alpha, i) - F_z\sin\alpha = 0 \qquad (12)$$

where F_z is simply a sixth of the total vehicle load. Considering the non-linear nature of the drawbar vs. slip vs. normal load surfaces, approaches 2 and 3 are expected to produce different results.

Results of Scarecrow climbing capabilities are presented in Figure 10. Full vehicle simulations conducted with ARTEMIS are capable of accurately describing slope climbing capabilities of the rover. The approaches 2 and 3 are also able to produce predictions close to the actual rover performance. This is an interesting result because it shows that, for the rover configuration, soil type, and range of wheel slip considered here, it is possible to use single wheel experiments conducted on flat ground to estimate the performance of a full MSL vehicle without the need of knowing the vertical load distribution among the axles.

Table 3. Sand properties for the Dumont Dunes site obtained from ARTEMIS simulations.

Symbol	Value	Units
ρ	1650	kg/m^3
n_0	1.45	n/a
n_1	0.45	n/a
k_c'	9.1	n/a
k_ϕ'	500.8	n/a
c	200	Pa
ϕ	30	deg
k_x	0.029	m
a_1	0.33	n/a
a_2	0.11	n/a

6 Conclusions

This paper presented recent work toward developing a terramechanics-based modeling and validation infrastructure for characterizing the Curiosity rovers mobility prop-

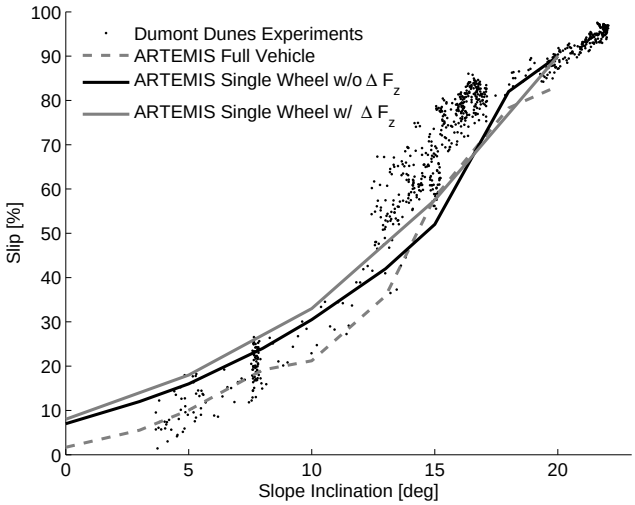

Figure 10. Scarecrow climbing characteristics at the Dumont Dunes site.

erties on the Mars surface. The Adams-based simulator ARTEMIS was utilized to reproduce single wheel experiments conducted at MIT and full vehicle experiments conducted at the Dumont Dunes site.

The results show that it is possible to utilize single wheel simulations conducted on flat terrain to quickly estimate rover climbing capabilities. It should be noted that it was unfortunately not possible to perform experimental single-wheel tests on soil gathered from the Dumont Dunes site. For this reason, ARTEMIS simulations of single-wheel tests were used to predict upslope driving performance.

ARTEMIS is intended to be used on a continuing basis as a tool to help evaluate mobility issues over candidate Mars Science Laboratory Curiosity rover drive paths. The model will be employed to help plan drives for Curiosity, providing a set of outputs to help the engineers analyze routes to desired target sites that minimize wheel sinkage and slip, and thus minimize the probability of embedding. In addition, ARTEMIS enables the possibility of retrieving Mars soil, bedrock and topographic properties, by iterative registration of model outputs against actual drive results.

Acknowledgment

This work was supported by contracts from the Jet Propulsion Laboratory through the Mars Exploration Rover and Mars Science Laboratory missions. The authors gratefully acknowledge the work of the field crew, led by Matthew Heverly, who conducted the tests at the Dumont Dunes site, and Thuan Doan and Gregory Puszko for their help in designing and fabricating the terramechanics test bed at MIT.

References

[1] R. E. Arvidson, J. W. Ashley, J. F. Bell, M. Chojnacki, J. Cohen, T. E. Economou, W. H. Farrand, R. Fergason, I. Fleischer, P. Geissler, R. Gellert, M. P. Golombek, J. P. Grotzinger, E. A. Guinness, R. M. Haberle, K. E. Herkenhoff, J. A. Herman, K. D. Iagnemma, B. L. Jolliff, J. R. Johnson, G. Klingelhfer, A. H. Knoll, A. T. Knudson, R. Li, S. M. McLennan, D. W. Mittlefehldt, R. V. Morris, T. J. Parker, M. S. Rice, C. Schrder, L. A. Soderblom, S. W. Squyres, R. J. Sullivan, and M. J. Wolff. Opportunity mars rover mission: Overview and selected results from purgatory ripple to traverses to endeavour crater. *Journal of Geophysical Research: Planets*, 116(E7):n/a–n/a, 2011.

[2] R. E. Arvidson, P. Belutta, F. Calef, A. A. Fraeman, J. Garvin, O. Gasnault, J. Grant, J. Grotzinger, V. Hamilton, M. Heverly, K. Iagnemma, J. Johnson, N. Lanza, S. Le Mouelic, N. Mangold, D. Ming, M. Mehta, R. V. Morris, H. Newsom, N. Renno, D. Rubin, J. Schieber, R. Sletten, A. R. Vasavada, J. Vizcaino, and R. C. Wiens. Terrain physical properties derived from orbital data and the first 360 sols of mars science laboratory curiosity rover observations in gale crater. *J. Geophys. Res. - Planets*, in review.

[3] M. G. Bekker. *Introduction to Terrain-Vehicle Systems*. The University of Michigan Press, Ann Arbor, 1969.

[4] Liang Ding, Hai-bo Gao, Zong-quan Deng, and Jianguo Tao. Wheel slip-sinkage and its prediction model of lunar rover. *Journal of Central South University of Technology*, 17(1):129–135, 2010.

[5] J. P. Grotzinger, J. Crisp, A. R. Vasavada, R. C. Anderson, C. J. Baker, R. Barry, D. F. Blake, P. Conrad, K. S. Edgett, B. Ferdowski, R. Gellert, J. B. Gilbert, M. Golombek, J. Gmez-Elvira, D. M. Hassler, L. Jandura, M. Litvak, P. Mahaffy, J. Maki, M. Meyer, M. C. Malin, I. Mitrofanov, J. J. Simmonds, D. Vaniman, R. V. Welch, and R. C. Wiens. Mars science laboratory mission and science investigation. *Space Science Reviews*, 170(1-4):5–56, 2012.

[6] Matt Heverly, Jaret Matthews, Justin Lin, Dan Fuller, Mark Maimone, Jeffrey Biesiadecki, and John Leichty. Traverse performance characterization for the mars science laboratory rover. *Journal of Field Robotics*, 30(6):835–846, 2013.

[7] K. Iagnemma, H. Shibly, and S. Dubowsky. A laboratory single wheel testbed for studying planetary rover wheel-terrain interaction. *MIT Field and*

Space Robotics Laboratory Technical Report, 1:05–05, 2005.

[8] C. Senatore and K. Iagnemma. Direct shear behaviour of dry, granular soils subject to low normal stresses. In *Proceedings of 17th International Conference of the ISTVS*, Blacksburg, VA, 2011.

[9] C. Senatore and K. Iagnemma. Analysis of stress distributions under lightweight wheeled vehicles. *Journal of Terramechanics*, 51(0):1 – 17, 2014.

[10] J. Y. Wong. *Terramechanics and Off-Road Vehicle Engineering*. Elsevier, UK, 2nd edition, 2010.

[11] F. Zhou, R. E. Arvidson, K. Bennett, B. Trease, R. Lindemann, P. Bellutta, K. Iagnemma, and C. Senatore. Simulations of mars rover traverses. *Journal of Field Robotics*, 31(1):141–160, 2014.